

Modeling of Tissues *in vivo* Heating Induced by Exposure to Therapeutic Ultrasound

B. GAMBIN, E. KRUGLENKO, T. KUJAWSKA AND M. MICHAJŁOW

Institute of Fundamental Technological Research, Polish Academy of Sciences

A. Pawińskiego 5B, 02-106 Warsaw, Poland

The aim of this work is mathematical modeling and numerical calculation in space and time of temperature fields induced by low power focused ultrasound beams in soft tissue *in vivo* after few minutes exposure time. These numerical predictions are indispensable for planning of various ultrasound therapeutic applications. Both, the acoustic pressure distribution and power density of heat sources induced in tissue, were calculated using the numerical solution to the second order nonlinear differential wave equation describing propagation of the high intensity acoustic wave in three-layer structure of nonlinear attenuating media. The problem of the heat transfer in living tissues is modelled by the Pennes equation, which accounts for the effects of heat diffusion, blood perfusion losses and metabolism rate. Boundary conditions and geometry are chosen according to the anatomical dimensions of a rat liver. The obtained results are compared with those calculated previously and verified experimentally for temperature elevations induced by ultrasound in liver samples *in vitro*. The analysis of the results emphasizes the value of the blood perfusion and the values of heat conductivity on the temperature growth rate. The numerical calculations of temperature fields were performed using the ABAQUS FEM software package. The thermal and acoustic properties of the liver and water being the input parameters to the numerical model were taken from the published data in cited references. The range of thermal conductivity coefficient of living tissue is obtained from the model of two-phase composite medium with given microstructure. The first component is a "solid" tissue and the second one corresponds to blood vessels area. The circular focused ultrasonic transducer with a diameter of 15 mm, focal length of 25 mm and resonance frequency of 2 MHz has been used to generate the pulsed ultrasonic beam in a very introductory experiment *in vivo*, which has been performed. Numerical prediction confirms qualitatively its results.

PACS: 87.50.wp

1. Introduction

Theoretically, a properly tuned tempo-spatial temperature distribution in tissue would lead to desired heat shock response in the cells and, in consequence, enhanced expression of heat shock proteins which are important from the therapeutic point of view, see [1–4]. It is also important to assure that the increased temperature does not stimulate the ion activity within the cells and that the temperature itself is kept within the therapeutic range, i.e. up to 43 °C. In order to meet requirements mentioned above, ultrasonic technique may be applied, cf. [5–7], to ensure the non-invasive and strictly controlled heating of the target tissue volumes. Ultrasonic regimes can be controlled by adjusting the ultrasound beams intensity, frequency, pulse duration, duty-cycle and exposure time. The control of spatial temperature distribution is of essential importance for correlation between the level of temperature and the level of the gene expression. Furthermore, it is crucial to establish safe protocols for heat-responsive gene therapy in clinical applications.

In recent years, thanks to technical improvements of the focused ultrasound (a new generation of ultrasound transducers) has become possible to develop experimental studies on a precise local living tissues heating, not exceeding 43 °C.

In the intended therapy of a rat liver based on the ultrasound-guided heat shock proteins (HSP) expression enhancement the temperature rise in the liver should not exceed 6 °C above normothermia level of 37 °C.

Preliminary measurements of temperature rises induced in a rat liver *in vivo* by pulsed focused ultrasonic beam with the intensity of ISATA = 0.57 W/cm², generated from the circular transducer with a 2 MHz centre frequency, 15 mm diameter and 25 mm focal length have been carried out. The 20 cycle tone bursts with 20 duty-cycle penetrate the rat liver after passing through a water layer whose thickness is specific for the transducer considered and is determined theoretically. The temperature rise at the acoustic beam focus was measured using a thermocouple inserted within the liver of the rat under anesthesia. The experimental results obtained for the rat liver *in vivo* were compared with those for the fresh liver *in vitro* of the same rat while maintaining the same beam acoustic power and other experimental boundary condition parameters. The quantitative analysis of the obtained measurement results allowed to demonstrate that the temperature rise induced in the rat liver *in vivo* (when blood circulation in tissue vessels exists) is about 3 times lower than that induced in the fresh rat liver sample *in vitro* (without blood circulation) of the same rat. The most probable reason of that is higher thermal

conductivity of the rat liver *in vivo* (which shows a blood vessels area volume fraction of about 0.10–0.20) with respect to the sample of the fresh rat liver *in vitro*. The aim of the paper is to perform numerical simulation with such a data that the results confirm these phenomena.

Research on the prediction of living tissue temperature has been developed continuously since 1948, when Pennes [8] proposed a simple heat transfer model with a perfusion source term. Many other models were proposed, recently e.g. in [9] and references cited in [10], but the Pennes model might still be the best practical approach for modeling bio-heat transfer because of its simplicity.

Thermal properties of a living tissue differs from thermal properties of the dead tissue separated from the body. In the living tissue there exists a blood circulation as well as heat production due to metabolism. Since the experiment *in vitro*, described in [11], was performed on homogeneous (without large blood vessels) liver tissue samples it can be assumed that the chemical composition and structure of samples are similar to this area of tissue in the living organism, inside which acoustic irradiations are planned. Thermal processes in the living tissue, defined as a continuous material body, will be modeled in two ways.

Firstly, in the simplified Pennes equation, which has been used in [11] in numerical calculations of tissue heating process *in vitro*, we take into account two additional terms — perfusion term associated with the circulation of blood in vessels (cooling) and a term taking into account metabolic heat production (heating). It means that we deal with full classical Pennes equation.

Secondly, the coefficient of thermal conductivity of the tissue is assumed to be considerably higher than it was assumed in numerical calculations of the samples *in vitro*. Its value, in the paper, is calculated as the effective (macroscopic) thermal conductivity of two-component microinhomogeneous medium. One component is the tissue “solid” material, and the other one corresponds to blood vessels. Blood circulations in the living body is so efficient that the temperature inside the area occupied by vessels with blood is nearly constant. The method we use in the paper allows us to motivate higher values of thermal conductivity than it was assumed in the modelling of *in vitro* tissue heating process.

2. Homogenization of stationary heat equation with periodic coefficients

The method, called homogenization, see e.g. [12], consists, roughly speaking, in replacing the model of heterogeneous medium with a periodic or random structure by an equivalent model of homogeneous one. Equivalence is here understood in the sense that the solution to the initial-boundary value problem under consideration for inhomogeneous medium is “close” in some sense, to the solution to the related initial-boundary value problem for the equivalent homogeneous medium with effective, macroscopic properties.

Among various approaches of homogenization theory the variational Γ -convergence method, G -convergence method and the asymptotic technique e.g. [13, 14] can be mentioned, the latter being applied in this paper. In the paper [15] the asymptotic behaviour of a nonlinear dynamical boundary-value problem describing the bio-heat transfer in microvascular tissues was studied with the help of the homogenization method. The domain occupied by a tissue is an ϵ -periodic structure, consisting of two parts: a solid tissue part and small regions of blood vessels. In such a domain, a heat equation is considered with nonlinear sink and source terms and with a dynamical condition imposed on the boundaries of the blood zones, connected with blood perfusion. The limit equation, as $\epsilon \rightarrow 0$, is a new effective heat equation, with extra-terms coming from the influence of the non-homogeneous dynamical boundary conditions. In the effective, macroscopic heat equation the influence of the microstructure on effective coefficients, inter alia perfusion rate and effective conductivity, are demonstrated. The existence and uniqueness of a solution of the macro-model problem are proved, but no method of its solution has been suggested.

From the point of view of our modeling the most important question is how to take into account the influence of microstructure on the value of effective thermal conductivity of the living tissue. Below, we remind some classical homogenization asymptotic method used to obtain macroscopic thermal conductivity of the two-phase composite under the assumption that the region occupied by blood vessels is a component possessing higher by one or two orders of magnitude the conductivity than the “solid” tissue. This assumption is due to the blood perfusion in this region. We will use the Ritz method to calculate the effective, macroscopic conductivity and its quantity has been used in numerical finite element method calculations. Let $V \subset \mathbb{R}^3$ be a bounded regular domain and $\Gamma = \partial V$ its boundary. We introduce a parameter $\epsilon = \frac{l}{L}$, where l, L are typical length scales associated with microinhomogeneities and the region V , respectively.

We shall study the following linear transport equation [14]:

$$\begin{cases} -\frac{\partial}{\partial x_i} \left(a_{ij}^{(\epsilon)}(x) \frac{\partial u^{(\epsilon)}}{\partial x_j}(x) \right) = f(x), & x \in V, \\ u^{(\epsilon)}|_{\Gamma}(x) = 0, & x \in \Gamma, \end{cases} \quad (1)$$

where $a_{ij}^{(\epsilon)}(x) = a_{ij}(\frac{x}{\epsilon})$, $x \in V$. The second order tensor $\mathbf{A}^{(\epsilon)} = \{a_{ij}^{(\epsilon)}\}$, position vector $x = \{x_1, x_2, x_3\}$ and gradient vector $\nabla = \{\frac{\partial}{\partial x_1}, \frac{\partial}{\partial x_2}, \frac{\partial}{\partial x_3}\}$ in (1), are written in the fixed Cartesian basis of \mathbb{R}^3 . The tensor $\mathbf{A}^{(\epsilon)}$, in what follows, describes the anisotropic thermal conductivity properties of a microscopically inhomogeneous medium, in which the temperature field is identified with the scalar field $u^{(\epsilon)}$. The volume thermal sources f do not depend on the small parameter ϵ , so they are “macroscopic”. The

Dirichlet boundary conditions are stated, i.e. temperature is preserved on the boundary of volume V .

It must be underlined here that the effective, macroscopic thermal conductivity, in which we are interested, does not depend on the type of boundary conditions assumed, which is proved in [14]. We restrict here to the microstructure which are periodic. The limitations caused by this assumption are discussed in the book [12]. By Y we denote the so-called basic cell of periodicity, for instance $Y = (0, Y_1) \times (0, Y_2) \times (0, Y_3)$. For the sake of simplicity we assume that $a_{ij} = a_{ji}$, $i, j = 1, 2, 3$. As usual, we apply the summation convention i.e. repeated indices in bracket or not are summed. The material coefficients $a_{ij}(y)$ are Y -periodic in the first argument. More precisely

$$\begin{aligned} a_{ij} : (y) &\rightarrow a_{ij}(y), \\ \mathbb{R}^3 &\rightarrow \mathbb{R}, \end{aligned}$$

are assumed to satisfy the following conditions:

- (i) Functions $y \rightarrow a_{ij}(y)$ are measurable and Y — periodic functions.
- (ii) There exists a constant $\alpha > 0$ such that for $y \in Y$ almost every and for all $i, j = 1, 2, 3$ $|a_{ij}(y)| \leq \alpha$,
- (iii) There exists $\alpha_0 > 0$ such that

$$\begin{aligned} a_{ij}(y)\xi_i\xi_j &\geq \alpha_0|\xi|^2, \\ \text{for all } \xi &\in \mathbb{R}^3. \end{aligned}$$

We note that for a fixed $\epsilon > 0$ the material functions $a_{ij}^{(\epsilon)}(x) = a_{ij}(\frac{x}{\epsilon})$ are ϵY -periodic in V . After passage to the limit as $\epsilon \rightarrow 0$, the homogenized coefficients a_{ij}^e will be obtained.

3. Method of two-scale asymptotic expansions

According to this method we make the following assumption (*ansatz*):

$$u^{(\epsilon)}(x) = u^{(0)}(x, y) + \epsilon u^{(1)}(x, y) + \epsilon^2 u^{(2)}(x, y) + \dots \quad (2)$$

where $y = \frac{x}{\epsilon}$, and the functions $u^{(0)}(x, \cdot)$, $u^{(1)}(x, \cdot)$, $u^{(2)}(x, \cdot)$, etc. are Y -periodic. The upper indices in brackets (0), (1), ... are used here to denote the enumeration of the sequence in the expansion. In what follows we preserve the convention that the brackets in indices will denote enumeration of some sequences, they are not connected with any representation in the basis of geometrical objects. Tacitly it is assumed that all derivatives appearing in the procedure of asymptotic homogenization make sense. We recall that for a function $f(x, y)$, where $y = \frac{x}{\epsilon}$, the differentiation operator $\frac{\partial}{\partial x_i}$ should be replaced by $\frac{\partial}{\partial x_i} + \frac{1}{\epsilon} \frac{\partial}{\partial y_i}$. According to the method of asymptotic expansions we compare the terms associated with the same power of ϵ . The local functions $\chi^{(k)}(y)$, $k = \{1, 2, 3\}$, are

solutions to the so-called local problem

$$\frac{\partial}{\partial y_j} \left[a_{ij}(y) \left(\frac{\partial \chi^{(k)}(y)}{\partial y_i} + \delta_{ik} \right) \right] = 0. \quad (3)$$

Let us introduce the space of Y -periodic functions defined by: $\phi \in H_{\text{per}}(Y)$ if $\phi \in H^1(Y)$ and ϕ assumes equal values at the opposite faces of Y . $H^1(Y)$ denotes, as usual, the Hilbert space of square integrable, together with their first derivatives, functions defined over the domain Y .

The weak (variational) formulation of (3) reads: find $\chi^{(k)}(\cdot) \in H_{\text{per}}(Y)$ such that

$$\int_Y \left[a_{ij}(y) \left(\frac{\partial \chi^{(k)}(y)}{\partial y_i} + \delta_{ik} \right) \right] \frac{\partial v(y)}{\partial y_j} dy = 0, \quad (4)$$

for each $v \in H_{\text{per}}(Y)$. Then the homogenized equation has the following form:

$$-\frac{\partial}{\partial x_j} \left(a_{ij}^{(e)}(x) \frac{\partial u^{(0)}}{\partial x_i} \right) = f, \quad (5)$$

where the homogenized (upper index (e) — effective) coefficients are given by

$$a_{ij}^{(e)} = \frac{1}{|Y|} \int_Y \left[a_{ij}(y) + a_{kj}(y) \frac{\partial \chi^{(i)}}{\partial y_k} \right] dy. \quad (6)$$

In the case of the heat conduction $u^{(0)} = T$, where T is the macroscopic temperature.

The Ritz method, see e.g. [16], offers a possibility of the determination of local functions in an approximate manner. We shall be looking for an approximate solution of the local problem by the method. We take

$$\chi^{(m)}(y) = \chi_{(a)}^{(m)} \phi^{(a)}(y) = \sum_a \chi_{(a)}^{(m)} \phi^{(a)}(y). \quad (7)$$

Here $\phi^{(a)}(y)$, $a = 1, 2, \dots, \bar{a}$ are prescribed Y -periodic functions (shape functions) and $\chi_{(a)}^{(m)}$ are unknown constants.

The local problem (4) should now be satisfied for the test functions of the form

$$v = v_{(a)} \phi^{(a)}(y). \quad (8)$$

To determine the unknown constants one has to solve the following algebraic equations:

$$\chi_{(a)}^{(m)} A^{ab} = B^{mb}, \quad (9)$$

where

$$A^{ab} \equiv \int_Y a_{ij}(y) \phi_{,i}^{(a)} \phi_{,j}^{(b)} dy,$$

$$B^{ja} = - \int_Y a_{ji}(y) \phi_{,i}^{(a)} dy,$$

with $\phi_{,i}^{(a)} = \frac{\partial \phi^{(a)}}{\partial y_i}$. The solution reads as

$$\chi_{(a)}^{(k)} = (\mathbf{A}^{-1})_{ab} B^{kb}.$$

Here \mathbf{A}^{-1} is the inverse matrix of \mathbf{A} .

We finally obtain

$$a_{ij}^e = \langle (a_{ij}(y)) \rangle + (A^{-1})_{ab} B^{ib} B^{ja}. \tag{10}$$

To apply the outlined general procedure we consider a two-phase composite material with the conductivity coefficients given by

$$a_{ij}(y) = \begin{cases} \lambda_1 \delta_{ij} & \text{if } y \in Y_1, \\ \lambda_2 \delta_{ij} & \text{if } y \in Y_2. \end{cases} \tag{11}$$

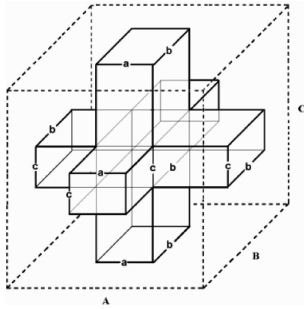


Fig. 1. Periodic geometry of interpenetrating network.

The microstructure that was used in the Ritz procedure (Maple 6) is depicted in Fig. 1. The periodic geometry forms so-called interpenetrating network. The volume fraction of vessels region was 0.1 and the values of conductivities in vessels region were assumed in the range 20–200 W/(m K). The results were used as data in FEM calculation of heat transport described by the Pennes equation introduced in the next section.

4. Model of bioheat transfer process

Bioheat transfer equation in two-phase medium, occupying domain V , Fig. 2 in the 3D real space (Pennes' equation for biological tissue), may be written as

$$\rho(x)C(x)\frac{\partial T(x,t)}{\partial t} = \nabla K(x)\nabla T(x,t) + Q_p(x,t) + Q_{\text{int}}(x,t) + Q_{\text{ext}}(x,t), \tag{12}$$

for $x \in V$, where T , t , ∇ , ρ , K , Q_p , Q_{int} , Q_{ext} denotes temperature, time variable, gradient vector, density, specific heat, thermal conductivity of a medium, which in the general case of anisotropic heat transfer is 2nd order tensor, perfusion, internal heat generation and external heating, here by ultrasonic irradiation processes, respectively, see [11]. In our case, coefficients in Eq. (12) are scalars (isotropic heat transfer) and constant on the prescribed regions, so we have

$$\rho(x) = \begin{cases} \rho_w & \text{for } x \in V_w, \\ \rho_t & \text{for } x \in V_t, \end{cases}$$

$$C(x) = \begin{cases} C_w & \text{for } x \in V_w, \\ C_t & \text{for } x \in V_t, \end{cases}$$

$$K(x) = \begin{cases} K_w & \text{for } x \in V_w, \\ K_t & \text{for } x \in V_t. \end{cases}$$

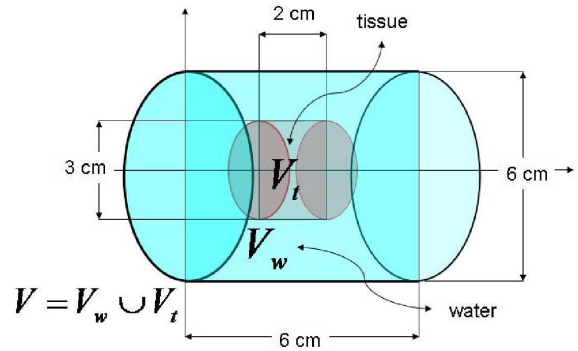


Fig. 2. Geometry of the problem.

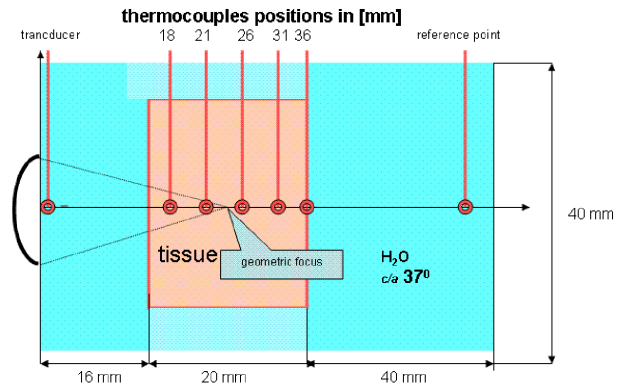


Fig. 3. Experiment *in vitro*.

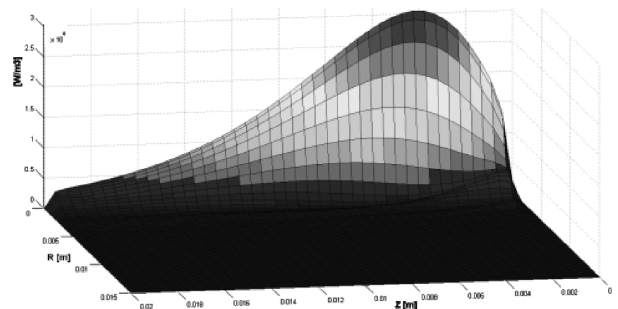


Fig. 4. Heat power density distribution.

The distribution of heat power sources induced in the tissue, denoted by Q_{ext} in (12), due to the acoustic pressure distribution, were calculated using the numerical solution to the second order nonlinear differential wave equation describing propagation of the high intensity acoustic wave in three-layer structure of nonlinear

attenuating media. The 3 layers are water, tissue and water, respectively, starting from transducer surface along the beam axis with the width 16 mm, 20 mm, 40 mm, noted in Fig. 3. The numerical data in the form of 2D matrix, next used in the FEM calculations was obtained by courtesy of J. Wójcik from Department of Ultrasounds in the Institute of Fundamental Technological Research. The shape of the distribution of heat power sources density inside the tissue is depicted in Fig. 4. To use the 2D matrix data in FEM an extra tool (script) was written, see Appendix. The value of the term Q_{int} was taken from literature as well as a term responsible to perfusion, namely Q_p .

5. Numerical results and conclusions

Abaqus 6.9 software (DS Simulia Corp.) was used to solve the problem formulated above. In the experiments the total sound power on the transmitter was equal to 1 W. It was calculated that the total power of heat sources

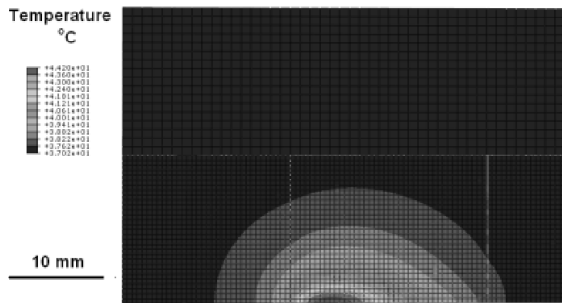


Fig. 5. Temperature pattern along beam axis after 600 s of irradiation.

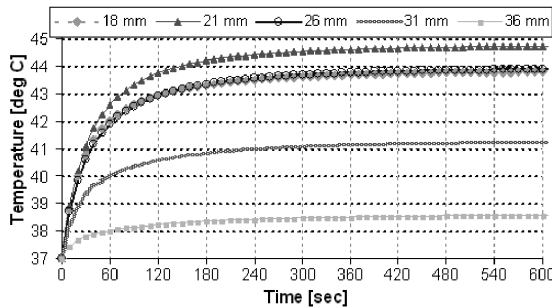


Fig. 6. Temperature rise in different distances from the transducer.

due to beam irradiation is equal to 0.654 W. At first, we have calculated the temperature rise due to the acoustic irradiation inside the tissue *in vitro* using now the more realistic, compared with the first approximation to heat sources homogeneous distribution proposed in our paper [11], inhomogeneous distribution of acoustic power, cf. Fig. 4, directly connected with the acoustic field converted into heat. The value and the rate of temperature rise of the tissue *in vitro* predicted by the model

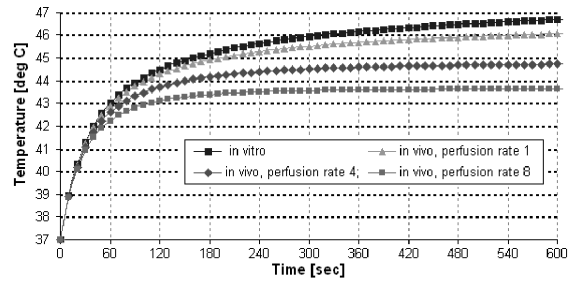


Fig. 7. Temperature rise without perfusion and for different perfusion rates with fixed conductivity (“solid” tissue conductivity).

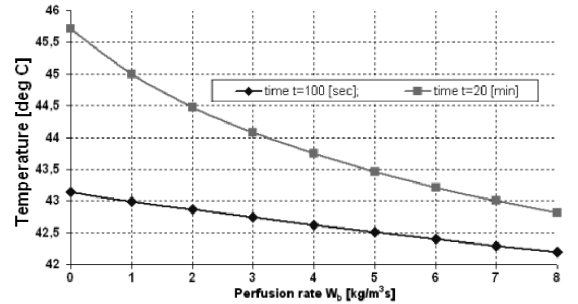


Fig. 8. Temperature level in the focus point versus different perfusion rates.

is pretty well confirmed by experiment, performed in Department of Ultrasounds and discussed in [11] — measurements done with thermocouples. A scheme of the performed experiment *in vitro* is shown in Fig. 3. The temperature pattern along the beam axis after 10 min of irradiation is illustrated in Fig. 5, while the temperature rises during 10 min of irradiation in different distances from transducer are depicted in Fig. 6. The shape and the intensity of temperature rise correspond to the inhomogeneous distribution of acoustic power due to the applied acoustic beam. Next, the temperature changes versus time up to 10 min of irradiation were calculated, taking into account different values of perfusion rate and fixed value of metabolic heat sources.

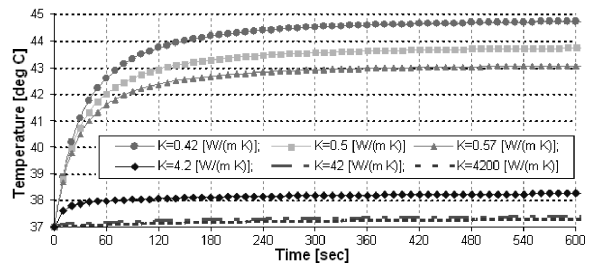


Fig. 9. Temperature rise in the focus point for different values of thermal conductivity.

TABLE

Material properties of water, tissue and blood used in numerical calculation.

Material	Water	Tissue	Blood
density [kg/(m ³)]	$\rho_w = 1000$	$\rho_t = 1060$	$\rho_b = 1000$
specific heat [J/(kg K)]	$C_w = 4200$	$C_t = 3600$	$C_b = 3800$
conductivity [W/(m K)]	$K_w = 0.6$	$K_t = 0.42\text{--}0.57$	$K_b = 0.6$

In Fig. 7 the results are demonstrated. It is clear that the perfusion (even for the highest numerical value reported in [17, 18]) does not decrease the temperature level sufficiently, while the conductivity coefficient is preserved being constant, cf. its numerical value from [11] is given in Table. In Fig. 8 temperature rises in the focus point for different perfusion rates are presented. At the end, we use the numerical values of effective conductivities resulting from the Ritz method calculation for interpenetrating network of blood vessels in the “solid” tissue. The temperature rise in the focus point after 10 min of irradiation is 3 times less than *in vitro* case for the predicted higher value of effective conductivity coefficient, cf. Fig. 9. We conclude at the end that the Pennes bioheat transport equation is adequate to analyse the thermal processes in living tissues if the effective properties of a composite microstructure of the tissue — even modelled by the periodic microstructure — are taken into consideration. The future FEM analysis will take into account the temperature dependence of acoustic properties of the tissue. It means that during the irradiation process the thermal sources will be changed. The experiments *in vivo* are also planned so their results should give sufficient information to verify our numerical predictions.

Appendix

This script had been written because of lack of appropriate abaqus internal tool. Its job is to apply a time invariant, spatially distributed body heat flux (BHF) in the specified body (here the liver tissue), on the basis of test data enclosed in form of a two-dimensional matrix. Below, there is a short description of implemented algorithm.

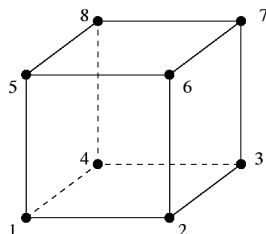


Fig. 10. Cubic element.

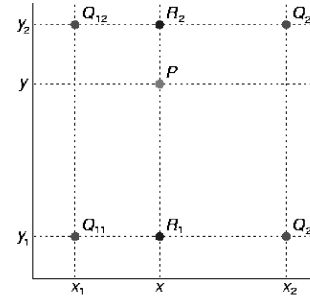


Fig. 11. Interpolation scheme.

1. Create node and element sets that belong to the heated body (liver).
2. Iterate through the set of elements. For each element:

- a. Compute its geometrical center (GC) coordinates. Use the fact that coordinates of element’s GC can be computed as average of the brick’s nodes coordinates, cf. Fig. 10:

$$x_c = \frac{1}{8} \sum_{i=1}^8 x_i, \quad y_c = \frac{1}{8} \sum_{i=1}^8 y_i,$$

$$z_c = \frac{1}{8} \sum_{i=1}^8 z_i.$$

- b. Transform the Cartesian coordinate system to cylindrical one. Because the considered model is treated as axisymmetrical, only two dimensions are needed in the new coordinate system — (z, r) .
- c. Compute the magnitude of BHF. If element’s GC coincide with any node of BHF input matrix, then element’s magnitude is simply the value of BHF at pointed node. When none of nodes does coincide with element’s GC, use bilinear interpolation method to compute the appropriate magnitude value, cf. Fig. 11,

$$f(x, y) \approx \frac{f(Q_{11})}{(x_2 - x_1)(y_2 - y_1)} \times (x_2 - x)(y_2 - y) + \frac{f(Q_{21})}{(x_2 - x_1)(y_2 - y_1)}$$

$$\begin{aligned} & \times (x_2 - x)(y_2 - y) + \frac{f(Q_{12})}{(x_2 - x_1)(y_2 - y_1)} \\ & \times (x_2 - x)(y_2 - y). \end{aligned}$$

3. Repeat 2nd step until the end of element set.

Acknowledgments

The authors acknowledge the Organizers of XVII Conference of Acoustical and Biomedical Engineering, Zakopane, Poland, March 22–26, 2010, for the possibility of presenting the lecture there. The authors were partially supported by the Polish Ministry of Science and Higher Education (grant no. N N518426936).

References

- [1] W.E. Balch, R.I. Morimoto, A. Dillin, J.W. Kelly, *Science* **319**, 916 (2008).
- [2] R. Morimoto, *Genes Dev.* **22**, 1427 (2008).
- [3] W. Walther, U. Stein, *Adv. Drug Delivery Rev.* **61**, 641 (2009).
- [4] A. Mizera, B. Gambin, *J. Theoret. Biol.* **265**, 455 (2010).
- [5] J. Wójcik, L. Filipczyński, *Ultrasound Med.* **30**, 99 (2004).
- [6] R.M. Arthur, W.L. Straube, J.W. Trobauch, E.G. Moros, *Int. J. Hyperthermia* **21**, 589 (2005).
- [7] I. Bazan, M. Vazques, A. Ramoz, A. Vera, L. Leija, *Ultrasonics* **49**, 358 (2009).
- [8] H.H. Pennes, *J. Appl. Physiol.* **1**, 93 (1948).
- [9] M.J. Daniels, J. Jiang, T. Varghese, *Ultrasonics* **48**, 40 (2008).
- [10] J.J. Telega, M. Stańczyk, in: *Modelling in Biomechanics*, Ed. J.J. Telega, Vol. 19, Institute of Fundamental Technological Research, Polish Academy of Sciences, Warsaw 2005, p. 191.
- [11] B. Gambin, T. Kujawska, E. Kruglenko, A. Mizera, A. Nowicki, *Arch. Acoust.* **34**, 445 (2009).
- [12] G. Milton, *Theory of Composites*, Cambridge University Press, Cambridge 2002.
- [13] G. Dal Maso, *An Introduction to Γ -convergence*, Birkhäuser, Boston 1993.
- [14] A. Bensoussan, J. Lions, G. Papanicolaou, *Asymptotic Analysis for Periodic Structure*, North Holland, Amsterdam 1978.
- [15] C. Timofte, *Acta Phys. Pol. B* **39**, 2811 (2008).
- [16] R. Courant, D. Hilbert, *Methods of Mathematical Physics*, Vol. 1, Interscience, New York 1953.
- [17] Z. Yuwen, *Int. J. Heat Mass Transfer* **52**, 4829 (2009).
- [18] Y. Ping, *Int. J. Heat Mass Transfer* **52**, 1734 (2009).